Texture characterization of dry-cured ham using multi energy X-ray analysis

E. Fulladosa, A. Austrich, I. Muñoz, L. Guerrero, J. Benedito, J.M Lorenzo, Gou, P.

IRTA. XARTA. Food Technology programme. Finca Camps i Armet, s/n 17121 Monells, Girona, Catalonia.

CTC. Centro Tecnológico de la Carne, Rúa Galicia Nº4, Parque Tecnológico de Galicia, San Cibrán das Viñas, 32900 Ourense, Spain.

UPV. Department of Food Technology, Universitat Politècnica de València, Camí de Vera s/n, E-46022 València, Spain.

Abstract – Multi energy X-ray sensors are able to differentiate and quantify X-rays of different energies. In contrast to conventional sensors, which simply record the overall energy of the X-rays whatever the energy of x-rays is, multi energy sensors provides a spectrum of the X-rays energies, which may be differently attenuated. In this study, the feasibility of this technology to detect changes in dry-cured ham slices after inducing proteolysis was evaluated. Effect of salt and water contents on the attenuation was also studied. In addition, the classification of commercial samples according to their proteolysis index was assessed. Results showed a decrease of attenuation for increasing proteolysis induction times ($p<0.01$) for all the regions of the spectrum (energy bands), but not with the same intensity, at any of the analysed acquisition conditions. Salt and water contents produced a significant ($p<0.01$) effect on the attenuation. Influence of salt content was higher than that of water content, and both affected the prediction of the proteolysis index. Classification score of commercial samples exhibited a limited discrimination capacity, showing the need for more sophisticated data analysis.

Key Words – non-destructive, quality evaluation, proteolysis, spectrometry

1. Introduction

Chemical and physical changes occur during the processing of dry-cured ham, impacting on the final texture of this product and influencing consumer's acceptability (Morales, Guerrero, Claret, Guàrdia, & Gou, 2008). These changes are strongly dependent on many factors such as the raw material characteristics, genetics, the activity of proteolytic enzymes and the processing conditions (Guerrero, et al., 2004; Schivazappa, et al., 2002; Skrlep, et al., 2011). The high variability of these factors and the complex interrelation between them make it difficult to control the correct development of the texture and gives rise to the development of texture defects such as pastiness, which is highly related to the proteolysis intensity of the samples and occurs in an important part of the dry-cured ham production (Tapiador Farelo & García Garrido, 2003). However, corrective treatments such as the application of mild thermal treatments (Morales, Arnau, Serra, Guerrero, & Gou, 2008) or high pressure (Fulladosa, Sala, Gou, Garriga, & Arnau, 2012) are able to reduce this defect. On this basis a rapid online method capable of non-destructive detection of product with defective textures would enable application of these corrective treatments prior to sale.

Several non-invasive technologies have the potential to determine textural features of dry-cured meat products (Damez & Clerjon, 2013; Font-i-Furnols, Fulladosa, Prevolnik, & Candek Potokar, 2015). In this regard, near infrared and microwave spectroscopy have been found able to discriminate between dry-cured hams with pastiness and those with a normal texture (García-Rey, García-Olmo, Pedro, Quiles-Zafra, & Castro, 2005; Ortiz, Sarabia, García-Rey, & Castro, 2006; Rubio-Celorio, Fulladosa, Claret, Guàrdia, & Garcia-Gil, 2013). Laser backscattering imaging has also been found to be related to the proteolysis index of hams but, as in the case of the previously mentioned technologies, many factors (especially water content) interfered with its estimation (Fulladosa, Rubio-Celorio, Skytte, Muñoz, & Picouet, 2017). X-ray based technologies, using single or dual absorptiometry, were proved to be useful for compositional analysis of thick samples of dry-cured ham (De Prados, et al., 2015; Fulladosa, et al., 2015) whereas salt content in sliced dry-cured ham could only be achieved using recently developed multi energy sensors (Fulladosa, Gou, & Muñoz, 2016). In contrast to conventional sensors, multi energy sensors are able to measure the energy of each transmitted photon and construct an energy spectra over several energy channels. Information provided by these spectra might be useful to analyze textural characteristics. However, no studies related to estimation of textural characteristics using this type of X-ray sensors were found in literature.

The aim of this work was to evaluate the feasibility of multi energy X-ray spectrometry to detect changes in sliced dry-cured ham after inducing proteolysis using a proteolytic enzyme. The effect of proteolysis and salt and water contents on X-ray attenuation at different acquisition conditions

was analysed. The ability of the technology to characterize and classify commercial samples according to their proteolysis index or defective texture level was also assessed.

2. Material and methods

2.1 Prototype device with multi energy X-ray detector

An X-ray system (MXV-MEAT 6025, Multiscan Technologies, Cocentaina, Spain) with a multi energy detector was used to scan the samples (Figure 1). The prototype had an X-ray spectrometric detector made of a semiconductor crystal (CDTe/CZT) with a pixel size of 0.8 mm. A belt conveyor transported the sample at a speed of 10 m/min. Simultaneously, X-rays were emitted from below the samples using a tungsten X-ray tube which operates from 40 to 150 kV. The energy of the transmitted X-rays was measured at the upper part of the device using the detector. The system acquired a spectroscopic image (1000 x 256 pixels) of the sample with each pixel containing an X-ray energy spectra of 128 channels (recording energies from 20 to 160 keV). The size of the acquired information was a 3D matrix consisting of 1000 x 256 pixels x 128 channels.

2.2 Extraction of ROI information: mean spectra and energy bands

In order to analyse the images, specific regions of interest (ROIs) from each sample, specifically *Biceps femoris* muscle, were selected. The selected ROIs, in which each pixel contained an energy spectrum, were analysed using a Matlab script written in house (MATLAB, Ver. 7.7.0, The Mathworks Inc., Natick, MA, USA). The mean X-ray attenuation (S_a) for the energy channel *a* of the selected ROI (Figure 2) was calculated after background correction and log-transformation as described in equation 1.

$$S_a = \frac{-\sum_{i=1}^{p} \ln\left(\frac{I_f^{a,i}}{I_o^{a,i}}\right)}{p} \qquad \text{(Eq 1)}$$

where I_f is the intensity of the transmitted radiation and I_o is the intensity of the incident radiation at each pixel *i* of the ROI which contains *p* pixels. The calculation was done for each energy channel *a*, which ranged from 1 to 128 and represented a given X-ray energy. According to Eq 1, an increase of S_a value represents an increase of the X-ray attenuation for channel *a*.

There was a part of the spectra in which photons with energies higher than the maximum applied keV were found. This was due to the pile up phenomenon (McCollough, Leng, Yu, & Fletcher, 2015) and it was not included in the analysis.

Different Energy bands (EB) of the spectra, (*x*-*y*) being the given number of energy channels, were selected (Figure 2). Energy band attenuation was calculated as the average attenuation of the energy channels included in the energy band using equation 2;

$$EB_{x-y} = \frac{\sum_{a=x}^{y} S_a}{y-x+1} \qquad \text{(Eq. 2)}$$

x and *y* correspond to the first and last energy channel *a* of the energy band considered. In this study, energy bands investigated contained 20 channels resulting in the whole spectra being divided into 6 energy bands (Figure 2). Each energy band represents areas of the spectrum with different responses.

2.3 Experimental protocols

2.3.1 Effect of induced proteolysis on multi energy X-ray spectra and energy bands

The effect of sliced dry-cured ham exposure to a proteolytic enzyme on the X-ray spectra when using different acquisition conditions (140 kV and 1 mA, 110 kV and 1.5 mA, 80 kV and 2.8 mA) was evaluated. For this purpose, 22 commercial dry-cured ham packages of approximately 240 g (12 slices each) were used. Proteolysis was induced by spreading 0.125 mL of a proteolytic enzyme (Delvolase®, DSM Food Specialties, France) on each face (about 90 cm^2) of the slices fromthe package. The slices were immediately piled and vacuum packaged again. This procedure facilitated the penetration of the enzyme and allowed a more homogeneous proteolysis generation in the package. Samples were kept vacuum packaged at 25ºC to induce proteolysis and were scanned after 0, 2, 4, 6, 8, 24 and 48h. According to Rubio et al (2013), increase of the proteolytic induction time will produce a logarithmic increase of pastiness or defective texture level.

From each acquired spectroscopic image, the *Biceps femoris* (BF) muscle was manually selected and the mean attenuation spectrum (Eq. 1) for each energy band (Eq. 2) was calculated. Afterwards, salt and water contents of the BF muscle were then analytically determined.

2.3.2 Characterization of dry-cured ham slices using multi energy X-ray spectra

160 dry-cured hams were measured to evaluate the feasibility of the technology to characterize or classify samples according to their proteolysis index. 160 raw hams with a pH<5.5, which are more prone to developing defective textures, were obtained from a commercial slaughterhouse. All the hams (n = 160) were weighed (11.9 kg ± 1.1 kg) and salted according to the traditional system; hams were manually rubbed with the following mixture (g/kg of raw ham): 0.15 of KNO_3, 0.15 of $NaNO_2$, 1.0 of dextrose, 0.5 of ascorbic acid and 10 of NaCl. The hams were pile salted at 3 ± 2 ºC and 85 ± 5% RH for 4 (n=40), 6 (n=40), 8 (n=40) or 11 days (n =40) to obtain samples with a broad range of salt content. After salting, hams were washed with cold water and post-salted at 3 ± 2 ºC and 85 ± 5% RH for 45 days. The hams were then submitted to a drying process at 12 ± 2 ºC and 70 ± 5% RH until reaching a weight loss of 29%. The hams were then vacuum packaged and kept at 30ºC for 30 days to induce proteolysis (breakage of proteins) and to promote samples with a broad range of proteolysis index (defined as the ratio between non protein nitrogen and total nitrogen). After this time, the drying process was continued at 12 ± 2 ºC and 65 ± 5%

RH until the hams reached a weight loss of 34%. The pieces were then vacuum packaged again and kept at 30ºC for 30 more days. After this period, the hams were dried again until the end of process (considered when a weight loss of 36% was reached). At the end of the process, the hams were boned and sampled.

2 cm thick slices from each ham were obtained and scanned at 110 kV and 1.5 mA (previously established as the optimal). A ROI containing the BF muscle was selected, the mean attenuation spectra was calculated as described in section 2.2 and pile up region discarded from the spectra. Subsequently, instrumental texture, salt and water contents and proteolysis index of the BF muscle were determined as described in section 2.4.

Samples were separated into different groups according to their proteolysis index, which is known to be related to a defective texture (Ruiz-Ramírez, Arnau, Serra, & Gou, 2006; Ruiz-Ramírez, Serra, Gou, & Arnau, 2006), for further statistical analysis. The following groups were defined: Standard, PI < 37% and high defective, PI > 37%.

2.4 Physicochemical and sensory analysis

Water content was analysed by drying at 103±2 ºC until reaching a constant weight (AOAC, 1990). Chloride content was determined according to ISO 1841-2 using a potentiometric titrator 785 DMP Titrino (Metrohm AG, Herisau, Switzerland) and expressed as salt content. Non-protein nitrogen content (NPN) was determined by precipitation of proteins with trichloroacetic acid (Kerese, 1984) followed by determination of the total nitrogen (TN) in the extract with the Kjeldahl method (AOAC, 2011). Proteolysis index (PI) was determined as a percentage of the ratio between NPN and TN (Careri, et al., 1993; Schivazappa, et al., 2002). All the analyses were performed in triplicate. Stress relaxation tests on BF muscles using parallelepipeds with the same dimensions (2 cm x 2 cm x 1.5 cm) were performed. Initial force F_0 (kg) (representing hardness) and force decay at 2 s (Y_2) and 90 s (Y_{90}) were calculated as previously described (R. Morales, Guerrero, Serra, & Gou, 2007). A sensory analysis to evaluate pastiness, adhesiveness and saliva viscosity was also carried out by an expert three-member panel trained following the American Society for Testing and Materials standards (ASTM, 1981).

2.5 Statistical analysis

In order to evaluate the effect of the proteolytic induction (closely related to proteolysis intensity) on the multi energy X-ray spectra, a two-way ANOVA was carried out including proteolytic induction time as main effect and sample as block effect. Analyses were performed on the following dependent variables: 1) attenuation of each channel of the spectra and 2) attenuation of the energy bands calculated from the spectra (section 2.2), when using different acquisition conditions. Differences between proteolytic induction times were tested by means of Tukey test. In order to study the influence of salt and water contents on the evaluation of proteolysis intensity,

an ANCOVA analysis was performed including proteolytic induction time as a fixed factor and salt and water contents as co-variables. Correlations between attenuation and salt and water contents at different energy bands were also determined by Pearson product-moment coefficient (r).

A partial least square regression (PLSR) analysis using all the channels of the spectra was performed to develop the predictive models for estimating the proteolysis index in the commercial ham samples. The 160 samples were split into two sets, 2/3 for the calibration (106 samples) and 1/3 for the validation (54 samples). To ensure a similar variation in composition in the calibration and validation sets, a stratified sampling method was performed. Coefficient of determination adjusted for degrees of freedom (R^2), standard error of calibration (RMSEC) and standard error of validation (RMSEV) were calculated. A partial least square regression coupled with a discriminant analysis (PLS-DA) was also used to determine the capacity of the model to distribute samples into defective and non-defective groups according to their proteolysis index level as established in section 2.3 and thus, to analyse the feasibility to separate highly defective textural samples. All the analyses were performed using the statistical package XLSTAT (Addinsoft, Paris, France).

3. Results

3.1 Effect of induced proteolysis on spectra and energy bands

Figure 3 shows the spectra of the intensity for the incident X-ray energies (dashed line) and the mean attenuation spectra for *Biceps femoris* muscle obtained from the sliced dry-cured ham after different proteolytic induction times (continuous lines) at different acquisition conditions.

At 140 and 110 kV, channels recording more than 1% of energy (channels from 1 to 48) accounted for 75% of the total intensity of the incident X-rays (Figures 3 a and b, dashed line) whereas at 80 kV, channels recording the total intensity of 85% were from 1 to 43 but the intensity of the incident energy per channel varied from 1 to 2.7%, increasing in the first channels and decreasing later on (Figure 3c, dashed line). As mentioned previously, the acquisition conditions (voltage and intensity of X-ray tube) can produce different attenuation responses (Fulladosa, et al., 2015; Håseth, et al., 2008) which may be more or less adequate to characterize or detect induced proteolysis. In the case of multi energy sensors, as shown in Figure 3, the spectra of the intensity for the incident X-ray energies influences the attenuation produced. The level of white noise in the image is lower in low energy channels. This fact could be attributed to the higher intensity of the incident X-rays at these energies in comparison to the rest of channels (the main part of X-rays have low energies). For this reason, information from the initial section of the spectra may provide more reliable information than that of the end part of the spectra.

At 140 and 110 kV a similar attenuation pattern and a minimum peak of attenuation was observed between channels 32 and 40 (energies 55 - 63 keV) (Figure 3a and 3b). In contrast, at 80 kV, a plateau of minimum attenuation was found between energy channels 20 and 40 (energies 41 - 63 keV) (Figure 3c). The attenuation response changed with the acquisition conditions, probably due to the different intensity pattern of incident energy. From energy channel 48 up to the last channel at 140 and 110 kV, and from 43 up to the last channel at 80 kV, information might be less reliable because of the high level of white noise in the images obtained at these energies probably caused by the lower amount of incident energy intensity. Information from the pile up region was not considered in the analysis (Figure 3, grey area). For sliced dry-cured ham (at any proteolytic induction times) attenuation clearly decreased with increasing X-ray energy as previously reported by other published works (Fulladosa, Santos-Garcés, Picouet, & Gou, 2010; Håseth, et al., 2008). However, an increase of attenuation was observed from energy channel 40 up to the end of the spectra. This fact may have been due to the insufficient intensity of the incident X-rays, as previously described, which starts to decrease steeply from this energy channel on. The attenuation of multi energy spectra clearly decreases when increasing proteolysis and degradation of the tissue, in the entire spectra and at all acquisition conditions (Figure 3). Statistical analysis showed a significant decrease of attenuation with increasing proteolytic induction times ($p<0.01$) for all the analysed energy channels and emission conditions. Grouping channel information in energy bands facilitated the comparison of the different regions of the spectra. At 140 kV, significant differences were observed among most proteolysis induction times and for all EB (Table 1). At 110 kV, the same previously described behaviour was observed (Table 2). However, acquisition at 110 kV was more discriminant than 140 kV since F values were higher. In contrast, at 80 kV (Table 3), no significant differences between 0 and 2 h, 4 and 6 h or 6 and 8 hours induction times were observed for any of the energy bands considered. It is still unknown what kind of phenomenon produce this decrease on attenuation. The attenuation of any material is basically caused by a combination of photo-electric and Compton effects. The photo-electric effect predominates at lower photon energies, is heavily energy dependant and is related to high atomic numbers. Compton scattering occurs almost independently of the photon energy at energies exceeding 30 keV and is predominantly related to the density of the material. Therefore, the observed decrease of attenuation could be attributed to the Compton scattering rather than the photo-electric effect. Changes on the scattering of X-rays due to the changes in the cell structure were suggested by Nielsen et al (2014) for frozen and defrosted fruit using dark-field radiography. Variations of X-ray scattering have also been observed in bovine muscle structure due to protein degradation using a small angle x-ray scattering synchrotron (Hoban, et al., 2016). Additionally, breaking of molecules and structures caused by proteolysis (Fulladosa, et al., 2017) might produce increased repulsion between molecules due to alteration in their molecular charges, and thus of

volume (not measurable) that could lead to a decrease of density in the sample and thus of attenuation.

3.2 Effect of sample composition on X-ray attenuation of induced proteolysis samples

The effect of dry-cured ham composition (salt and water content) on the X-ray attenuation has previously been reported previously for both dual energy (De Prados, et al., 2015; Fulladosa, et al., 2015) and multi energy sensors (Fulladosa, Gou, & Muñoz, 2016). Therefore, when analysing attenuation caused by proteolysis, sample compositions (salt and water contents) influence the spectra.

No significant correlation was found between salt and water contents (r=0.283) in the samples used to investigate the effect of proteolytic induction time. Statistical analysis of the effect of different proteolytic induction times using water and salt contents as co-variables (ANCOVA) showed a significant effect for both parameters in all the studied conditions. For all acquisition conditions (80, 110 and 140 kV) and energy bands, a negative slope for water was observed indicating that attenuation of spectra was negatively influenced by this parameter (an increase of water produced a decrease of attenuation). In contrast, attenuation was positively influenced by salt (an increase of salt produced an increase of attenuation). Because the slope value of salt content was higher than that of water content, the influence of salt content on the spectra is likely to be more relevant. For example, in the case of 110 kV, slope of salt content was 5.9, 3.2 and 2.7 times higher than that of water content for EB_{1-20}, EB_{21-40} and EB_{41-60}, respectively. However, it must be pointed out that the standard deviation of water content was 2.5 times higher than that of salt content, hence the influence of both parameters on X-ray attenuation for EB_{41-60} was similar.

Besides, before proteolysis was induced in the samples, the highest correlation of salt with attenuation (r=0.529) was found in EB_{1-20} at 80 kV as previously reported by Fulladosa et al (2016) and decreased for the other energy bands and acquisition conditions (Figure 4). For water, the correlation with attenuation was lower (r between -0.299 and -0.414) with similar values for the different acquisition conditions and energy bands. The lowest correlation for both salt and water contents was observed in EB_{20-41} at 110 kV. This result is in agreement with the low slopes of salt and water from ANCOVA analysis. Therefore, the region of the spectra with the least influence of salt and water is around channel 21 to 40 (X-ray energies between 43 and 64 keV) for emission conditions at 110 kV.

Other compositional variations and factors may significantly influence the acquired spectra. Moreover, proteolysis intensities obtained by using the proteolytic enzyme were higher than those found in commercial samples. For all these reasons, a validation using commercial-like samples is needed in order to study the feasibility of this technology for characterizing texture and/or detect textural defects in sliced dry-cured ham.

3.3 Characterization and classification of samples by partial least square regression and discriminant analysis

Prediction and classification feasibility of commercial samples according to their proteolysis index and defective texture was analysed using a PLSR and a PLS-DA analysis. As shown in Table 4, the proteolysis index and sensory pastiness intensity of the non-induced samples used in the study were significantly correlated (r=0.568) ($p<0.001$) (Table 4). Careri et al (1993) and Arnau (1991) have already described this fact. This allows the use of the proteolysis index as a chemical marker to characterize defective texture of dry-cured ham samples. Besides, proteolysis index of the samples was also significantly correlated to instrumental texture parameters (r=0.682 for Y_2, r=0.591 for Y_{90} and r=-0.636 for F_o). Morales et al (2007) described samples having low Y_{90} values as defective texture samples. In contrast, there was no correlation between the proteolysis index and salt (r=-0.031) or water contents (r=-0.008), despite proteolysis being sometimes related to a reduced salt content. The reason for this lack of correlation was the experimental design used as it aimed at obtaining samples with textural defects at different salt and water contents. This characteristic of the sample set is necessary to estimate the sample proteolysis index and evaluate the feasibility of the technology avoiding interference of composition (Fulladosa, et al., 2016).

Table 4 also shows the physicochemical characteristics of the samples used to develop PLSR models. A wide variation of proteolysis index ranging from 26.71 to 45.03 was obtained, as well as a wide variation of textural characteristics and salt and water contents. Developed PLSR models using spectra acquired at 110kV to predict the proteolysis index of the samples were not suitably robust. Figure 5 shows the RMSE of calibration and validation when using from 1 to 5 PLS factors. The minimum RMSE of calibration (3.16%) and validation (3.56%) were found when using two PLS factors showing a R^2 of 0.436. The use of more data might improve the robustness of predictive models.

The feasibility of discriminating samples in different groups using a PLS-DA model was also evaluated. Table 5 shows the physicochemical characteristics of high defective and standard samples sets. Significant differences of proteolysis index, F_o, Y_2 and Y_{90} between defined sets were obtained. Besides, the high defective set produced a decrease on the mean attenuation spectra in comparison to the standard set (Figure 6). This fact was attributed to the proteolysis index which was the only parameter significantly different between the two groups (Table 5). Using a PLS-DA model, the overall correct classification score for the validation data set was 75.93% when using 15 PLS factors. However, a limited discrimination power for the high defective samples was found, which obtained a classification correctness of only 44.44% (Table 6). This experiment should be evaluated using a higher number of samples in the defective group.

The use of more sophisticated algorithms, which for instance take into account the relation between several regions of the spectra, could also achieve better prediction results.

4. Conclusions

Multi energy X-ray analysis is able to detect changes caused by induced proteolysis in sliced dry-cured ham. The optimal acquisition conditions were 110 kV and 1.5 mA and changes were preferably detected in the low energy section of the spectra. Because of the important interference of salt and water contents on the X-ray attenuation, the ability of the technology to estimate or discriminate commercial samples according to the proteolysis index level is limited.

5. Acknowledgements

This work was partially supported by INIA (contract n. RTA2013-00030-CO3-01), Ministerio de Economia y Competitividad (PEJ-2014-A34573) and CERCA programme from Generalitat de Catalunya.

6. References

AOAC (1990). Official method 950.46, Moisture in meat, B. Air drying.

AOAC (2011). Official method 2011.04, Protein in Raw and Processed Meats.

Arnau, J. (1991). *Aportacions a la calidad tecnológica del jamón curado elaborado por procesos acelerados.* . Universitat Autònoma de Barcelona.

ASTM. (1981). American Society for Testing and Materials. Guidelines for the selection and training of sensory panel members. ASTM STP 758. In. ASTM, Philadelphia, p. 33.

Careri, M., Mangia, A., Barbieri, A., Bolzoni, L., Virgili, R., & Parolari, G. (1993). Sensory property relationships to chemical data of italian-type dry-cured ham. *Journal of Food Science, 58*(5), 968-972.

Damez, J.-L., & Clerjon, S. (2013). Quantifying and predicting meat and meat products quality attributes using electromagnetic waves: An overview. *Meat Science, 95*(4), 879-896.

De Prados, M., Fulladosa, E., Gou, P., Muñoz, I., Garcia-Perez, J. V., & Benedito, J. (2015). Non-destructive determination of fat content in green hams using ultrasound and X-rays. *Meat Science, 104*, 37-43.

Font-i-Furnols, M., Fulladosa, E., Prevolnik, M., & Candek Potokar, M. (2015). Future trends in non-invasive technologies suitable for quality determinations. In *A Handbook of Reference Methods for Meat Quality Assessment* (pp. 90-103). Brussels, Belgium: COST Action FA1102, FAIM.

Fulladosa, E., de Prados, M., García-Perez, J. V., Benedito, J., Muñoz, I., Arnau, J., & Gou, P. (2015). X-ray absorptiometry and ultrasound technologies for non-destructive compositional analysis of dry-cured ham. *Journal of Food Engineering, 155*, 62-68.

Fulladosa, E., Gou, P., & Muñoz, I. (2016). Effect of dry-cured ham composition on X-ray multi energy spectra. *Food Control, 70*, 41-47.

Fulladosa, E., Rubio-Celorio, M., Skytte, J. L., Muñoz, I., & Picouet, P. (2017). Laser-light backscattering response to water content and proteolysis in dry-cured ham. *Food Control, 77*, 235-242.

Fulladosa, E., Sala, X., Gou, P., Garriga, M., & Arnau, J. (2012). K-lactate and high pressure effects on the safety and quality of restructured hams. *Meat Science, 91*(1), 56-61.

Fulladosa, E., Santos-Garcés, E., Picouet, P., & Gou, P. (2010). Prediction of salt and water content in dry-cured hams by computed tomography. *Journal of Food Engineering, 96*(1), 80-85.

García-Rey, R. M., García-Olmo, J., Pedro, E., Quiles-Zafra, R., & Castro, M. D. L. (2005). Prediction of texture and colour of dry-cured ham by visible and near infrared spectroscopy using a fiber optic probe. *Meat Science, 70*, 357-363.

Guerrero, L., Gobantes, I., Oliver, M. A., Arnau, J., Guàrdia, M. D., Elvira, J., Riu, P., Grèbol, N., & Monfort, J. M. (2004). Green hams electrical impedance spectroscopy (EIS) measures and pastiness prediction of dry cured hams. *Meat Science, 66*, 289-294.

Håseth, T., Høy, M., Kongsro, J., Kohler, A., Sørheim, O., & Egelandsdal, B. (2008). Determination of sodium chloride in pork meat by computed tomography at different voltages. *Journal of Food Science, 73*(7), 333-339.

Hoban, J. M., Hopkins, D. L., Kirby, N., Collins, D., Dunshea, F. R., Kerr, M. G., Bailes, K., Cottrell, J. J., Holman, B. W. B., Brown, W., & Ponnampalam, E. N. (2016). Application of small angle X-ray scattering synchrotron technology for measuring ovine meat quality. *Meat Science, 117*, 122-129.

ISO 1841-2 (1996). Meat and Meat Products. Determination of Chloride Content -Part 2: Potentiometric Method (Reference method). Geneva: International Organization for Standardization

ISO 937:1978. Meat and meat products. Determination of nitrogen content (Reference method). International Organization for Standardization, Geneva.

Kerese, I. 1984. Methods of protein analysis. Chichester: Ellis Howood Ltd.

McCollough, C., Leng, S., Yu, L., & Fletcher, J. G. (2015). Dual- and Multi-Energy Computed Tomography: Principles, Technical Approaches, and Clinical Applications. *Radiology, 276*(3), 637-653.

Morales, Arnau, J., Serra, X., Guerrero, L., & Gou, P. (2008). Texture changes in dry-cured ham pieces by mild thermal treatments at the end of the drying process. *Meat Science, 80*, 231-238.

Morales, Guerrero, L., Claret, A., Guàrdia, M. D., & Gou, P. (2008). Beliefs and attitudes of butchers and consumers towards dry-cured ham. *Meat Science, 80*(4), 1005-1012.

Morales, R., Guerrero, L., Serra, X., & Gou, P. (2007). Instrumental evaluation of defective texture in dry-cured hams. *Meat Science, 76*, 536-542.

Nielsen, M. S., Christensen, L. B., & Feidenhans'l, R. (2014). Frozen and defrosted fruit revealed with X-ray dark-field radiography. *Food Control, 39*, 222-226.

Ortiz, M. C., Sarabia, L., García-Rey, R., & Castro, M. D. L. (2006). Sensitivity and specificity of PLS-class modelling for five sensory characteristics of dry-cured ham using visible and near infrared spectroscopy. *Analytica Chimica Acta, 558*, 125-131.

Rubio-Celorio, M., Fulladosa, E., Claret, A., Guàrdia, M. D. a., & Garcia-Gil, N. (2013). Detection of pastiness in dry-cured ham using dielectric time domain reflectometry. *59th International Congress of Meat Science and Technology - ICoMST 2013, Izmir, Turkey, 2013*.

Ruiz-Ramírez, J., Arnau, J., Serra, X., & Gou, P. (2006). Effect of pH24, NaCl content and proteolysis index on the relationship between water content and texture parameters in biceps femoris and semimembranosus muscles in dry-cured ham. *Meat Science, 72*, 185-194.

Ruiz-Ramírez, J., Serra, X., Gou, P., & Arnau, J. (2006). Efecto del índice de proteolisis sobre la textura del jamón crudo curado. *Archivos Latinoamericanos de Produccion Animal*, *14*(2), 62-64.

Schivazappa, C., Degni, M., Costa, L. N., Russo, V., Buttazoni, L., & Virgili, R. (2002). Analysis of raw meat to predict proteolysis in Parma ham. *Meat Science, 60*, 77-83.

Skrlep, M., Candek-Potokar, M., Mandelc, S., Javornik, B., Gou, P., Chambon, C., & Sante-Lhoutellier, V. (2011). Proteomic profile of dry-cured ham relative to PRKAG3 or CAST genotype, level of salt and pastiness. *Meat Science, 88*(4), 657-667.

Tapiador Farelo, J., & García Garrido, J. A. (2003). Avances en la ciencia, tecnología y comercialización del jamón (Cojamón 2003, Cáceres) In (pp. 70-77).

FIGURES

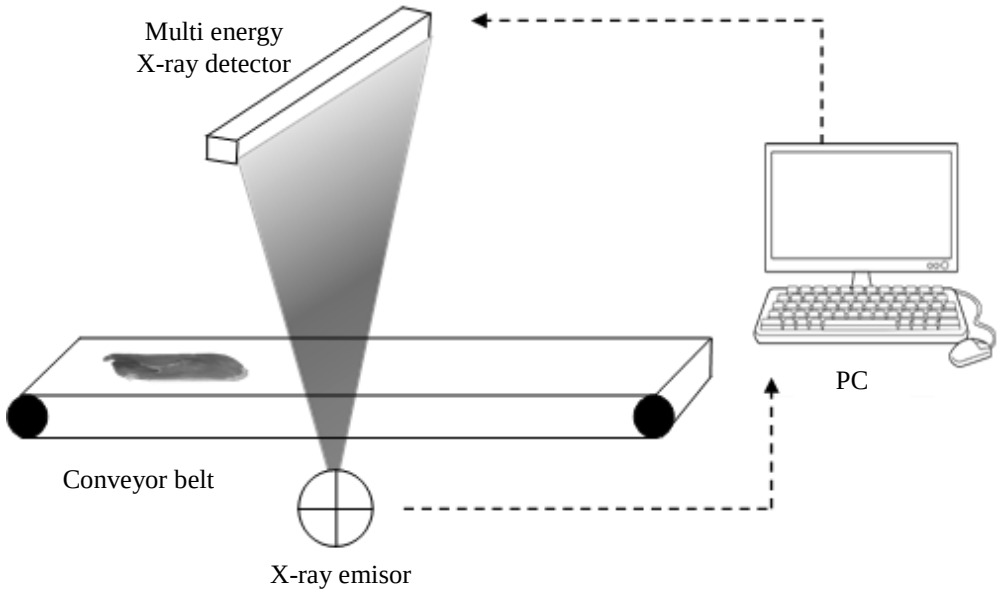

Figure 1. X-ray prototype system with a multi energy detector.

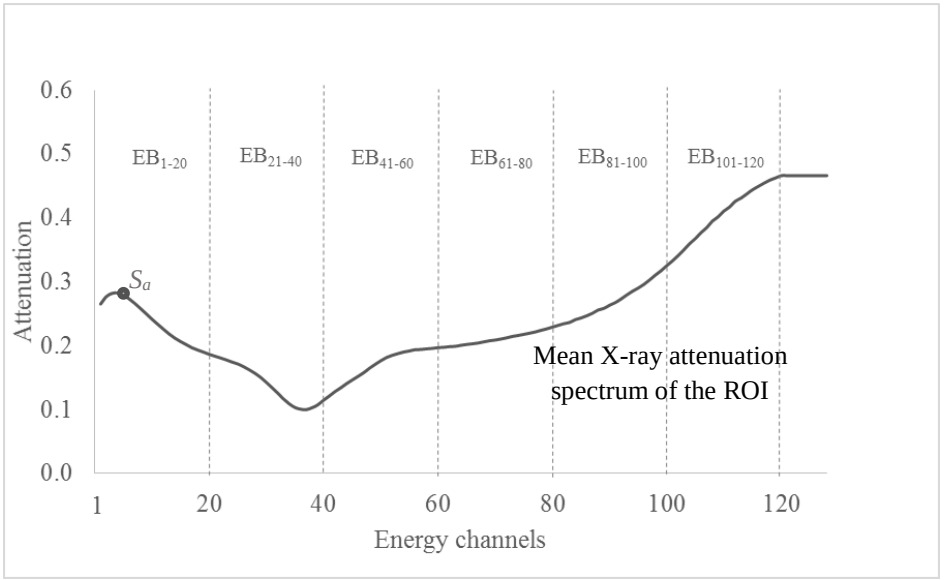

Figure 2. Representation of a mean X-ray attenuation spectrum of a ROI obtained by a multi energy X-ray device. EB: energy band; S_a: Attenuation value for a given energy channel *a*.

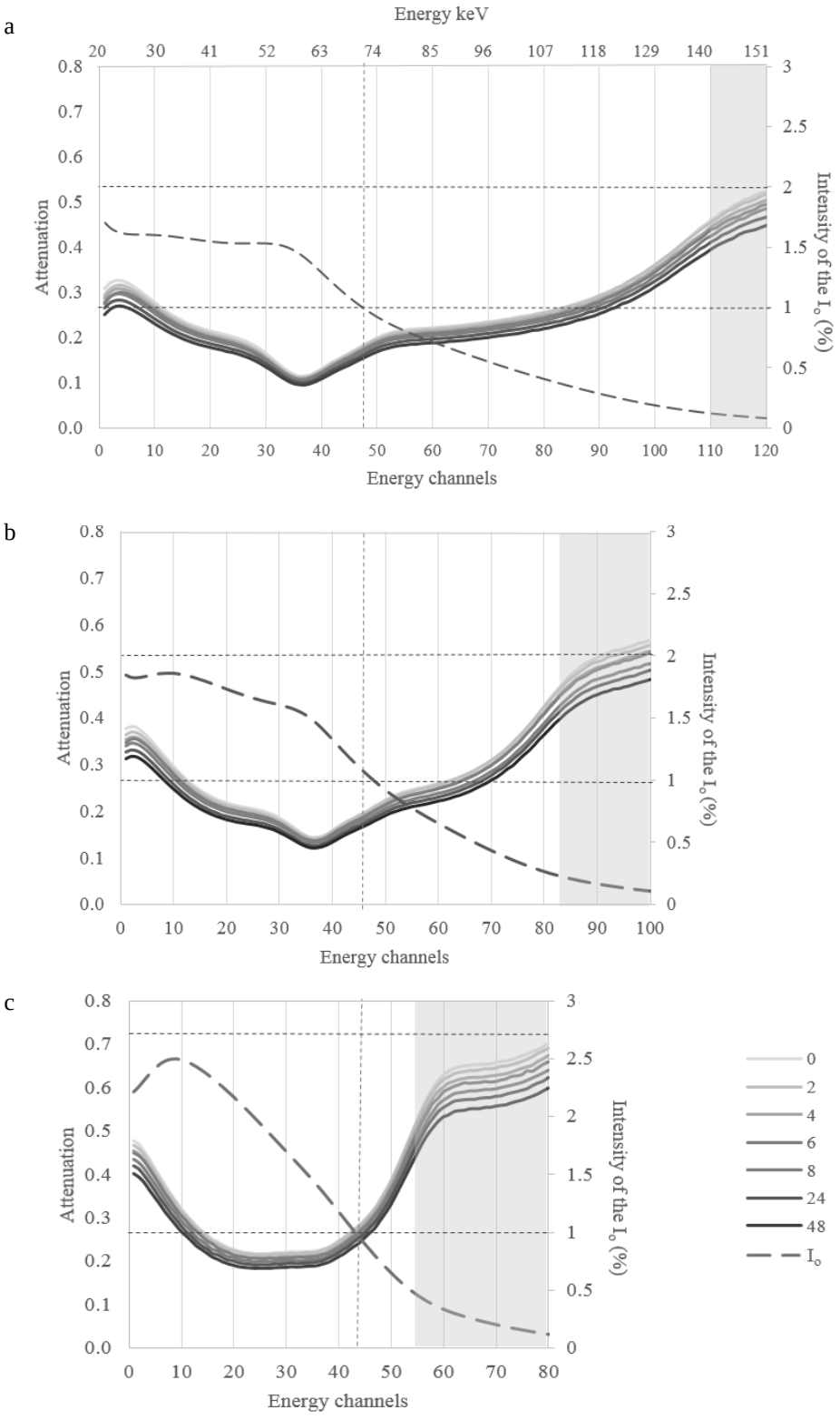

Figure 3. Mean X-ray attenuation spectra obtained from *Biceps femoris* muscle of sliced dry-cured ham after different proteolysis induction times (0, 2, 4, 6, 8, 24 and 48 h) when emitting at 140 kV and 1 mA (a), 110 kV and 1.5 mA (b) and 80 kV and 2.8 mA (c). Intensity of the incident X-rays of different energy (I_o) at the corresponding emission conditions is also showed. Grey area corresponds to pile up region.

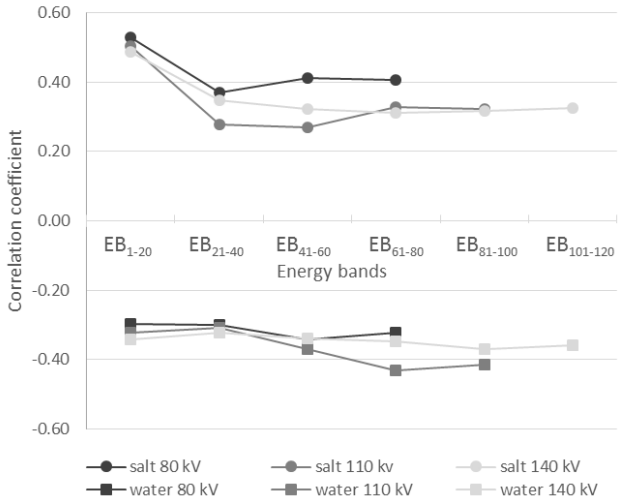

Figure 4. Correlation coefficients between attenuation and salt and water contents for the different energy bands when using spectra acquired from samples before proteolysis induction at different acquisition conditions (140, 110 and 80 kV).

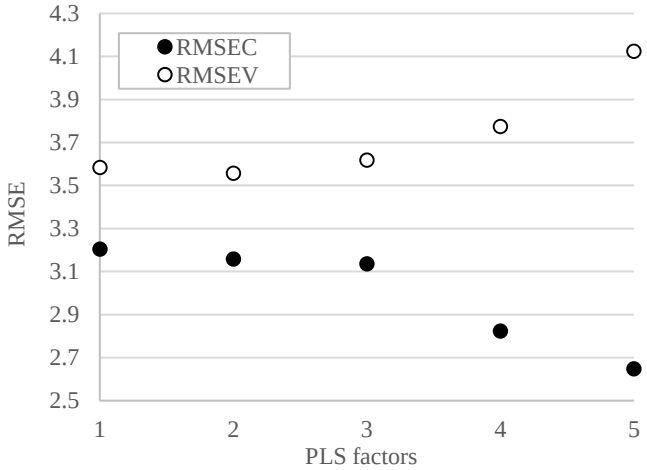

Figure 5. Variation of Root mean square errors (RMSE) for calibration and validation data sets when using different number of PLS factors.

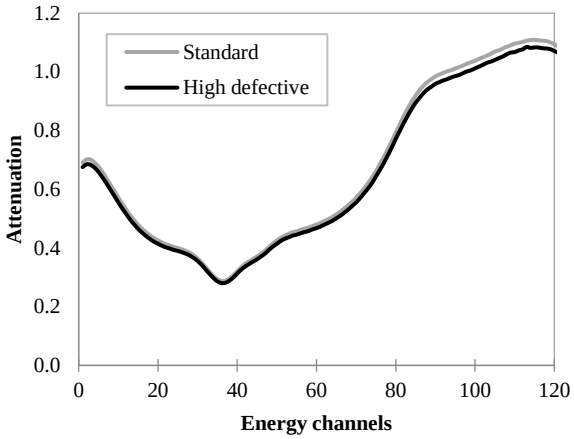

Figure 6. Mean X-ray attenuation spectrum for standard (IP<37%) and high defective (IP>37%) data sets acquired at 110 kV and 1.5 mA.

TABLES

Table 1. Mean and standard deviation of the attenuation for different energy bands of the spectra when emitting at 140 kV and 1 mA after different proteolysis induction times (n=22).

Time of enzyme exposure	EB_{1-20}		EB_{21-40}		EB_{41-60}		EB_{61-80}		EB_{81-100}	
	Mean	**SD**	**Mean**	**SD**	**Mean**	**SD**	**Mean**	**SD**	**Mean**	**SD**
0 h	0.272^{a}	0.044	0.160^{a}	0.037	0.192^{a}	0.030	0.237^{a}	0.018	0.301^{a}	0.036
2 h	0.266^{b}	0.043	0.156^{b}	0.036	0.190^{a}	0.030	0.235^{a}	0.018	0.300^{a}	0.037
4 h	0.259^{c}	0.042	0.152^{bc}	0.035	0.185^{b}	0.029	0.229^{b}	0.019	0.292^{b}	0.037
6 h	0.254^{cd}	0.042	0.149^{cd}	0.035	0.182^{bc}	0.030	0.225^{bc}	0.020	0.288^{b}	0.037
8 h	0.249^{d}	0.041	0.146^{d}	0.034	0.177^{c}	0.029	0.219^{c}	0.019	0.279^{c}	0.035
24 h	0.237^{e}	0.042	0.139^{e}	0.033	0.170^{d}	0.029	0.211^{d}	0.021	0.270^{d}	0.037
48 h	0.227^{f}	0.041	0.133^{f}	0.032	0.163^{e}	0.029	0.203^{e}	0.022	0.260^{e}	0.037

$^{a\text{-}f}$Different letters indicate significant differences ($p<0.05$) between proteolysis induction times within each calculated energy band. SD: Standard deviation; EB: Energy band.

Table 2. Mean and standard deviation of the attenuation for different energy bands of the spectra when emitting at 110 kV and 1.5 mA after different proteolysis induction times (n=22).

Time of enzyme exposure	EB_{1-20}		EB_{21-40}		EB_{41-60}		EB_{61-80}	
	Mean	**SD**	**Mean**	**SD**	**Mean**	**SD**	**Mean**	**SD**
0 h	0.297[a]	0.062	0.179[a]	0.028	0.221[a]	0.032	0.326[a]	0.054
2 h	0.289[b]	0.060	0.175[b]	0.027	0.218[a]	0.032	0.324[a]	0.055
4 h	0.282[c]	0.059	0.170[c]	0.027	0.212[b]	0.032	0.315[b]	0.054
6 h	0.278[c]	0.060	0.169[c]	0.028	0.210[b]	0.033	0.313[b]	0.054
8 h	0.270[d]	0.058	0.163[d]	0.027	0.202[c]	0.031	0.299[c]	0.051
24 h	0.258[e]	0.057	0.156[e]	0.027	0.195[d]	0.032	0.290[d]	0.053
48 h	0.248[f]	0.056	0.150[f]	0.026	0.188[e]	0.031	0.280[e]	0.051

[a-f]Different letters indicate significant differences ($p<0.05$) between proteolysis induction times within each calculated energy band. SD: Standard deviation; EB: Energy band.

Table 3. Mean and standard deviation of the attenuation for different energy bands of the spectra when emitting at 80 kV and 2.8 mA after different proteolysis induction times (n=22).

Time of enzyme exposure	EB_{1-20}		EB_{21-40}		EB_{41-60}	
	Mean	**SD**	**Mean**	**SD**	**Mean**	**SD**
0 h	0.332^{a}	0.087	0.224^{a}	0.017	0.419^{a}	0.129
2 h	0.326^{a}	0.085	0.220^{a}	0.017	0.416^{a}	0.126
4 h	0.317^{b}	0.083	0.214^{b}	0.017	0.405^{b}	0.124
6 h	0.315^{bc}	0.081	0.211^{bc}	0.013	0.396^{bc}	0.120
8 h	0.303^{c}	0.081	0.204^{c}	0.018	0.383^{cd}	0.118
24 h	0.290^{d}	0.080	0.196^{d}	0.020	0.374^{d}	0.117
48 h	0.278^{e}	0.078	0.189^{e}	0.021	0.359^{e}	0.113

$^{a\text{-}e}$Different letters indicate significant differences ($p<0.05$) between proteolysis induction times within each calculated energy band. SD: Standard deviation; EB: Energy band.

Table 4. Physicochemical characterization of non-induced samples used to develop and validate PLSR predictive models to determine proteolysis index as a biochemical indicator of dry-cured ham texture.

	Mean	Standard deviation	min	max	Pearson correlation coefficients						
					Proteolysis index (%)	Salt content (%)	Water content (%)	F_o	Y_2	Y_{90}	Pastiness perception
Proteolysis index (%)	34.79	3.71	26.71	45.03	1						
Salt content (%)	4.76	0.86	2.97	6.93	-0.181	1					
Water content (%)	58.89	0.98	55.98	61.76	-0.060	-0.397	1				
F_o	1.24	0.69	0.221	3.55	-0.634	0.278	-0.260	1			
Y_2	0.39	0.037	0.309	0.483	0.594	-0.168	0.168	-0.896	1		
Y_{90}	0.67	0.030	0.589	0.745	0.534	-0.262	0.213	-0.875	0.963	1	
Pastiness perception	1.25	1.39	0	6	0.568	-0.031	-0.008	-0.636	0.682	0.590	1

Table 5. Physicochemical characterization of high defective and standard texture groups used to develop and validate models to discriminate non-induced samples according to texture.

Sample set	n	Proteolysis index (%)				Salt content (%)		Water content (%)		F_0		Y_2		Y_{90}	
		Mean	SD	Min	Max	Mean	SD	Mean	SD	Mean	SD	Mean	SD	Mean	SD
High defective	29	40,04[a]	2,02	37,26	45,03	4,66	0,83	58,84	1,13	0,74[a]	0,37	0,42[a]	0,03	0,69[a]	0,03
Standard	134	33,16[b]	2,51	26,71	36,94	4,87	0,86	58,89	0,93	1,43[b]	0,67	0,38[b]	0,04	0,67[b]	0,03

[a-b]Different letters indicate significant differences ($p<0.05$) between high defective and standard set within each analysed parameter. SD: Standard deviation.

Table 6. Classification performance of standard and high defective dry-cured ham samples using PLS-DA.

	Standard	High defective	total	% Correctness
Standard	37	8	45	82.22
High defective	5	4	9	44.44
total	42	12	54	75.93